High−Throughput Measurement of Polymer Blend Phase Behavior

3 AUTHORS:

James Carson Meredith
Georgia Institute of Technology
107 PUBLICATIONS **2,474** CITATIONS

SEE PROFILE

Alamgir Karim
University of Akron
307 PUBLICATIONS **6,937** CITATIONS

SEE PROFILE

Eric Amis
University of Akron
181 PUBLICATIONS **6,508** CITATIONS

SEE PROFILE

High-Throughput Measurement of Polymer Blend Phase Behavior

J. Carson Meredith,*,† Alamgir Karim,* and Eric J. Amis*

Polymers Division, National Institute of Standards and Technology, Gaithersburg, Maryland 20899

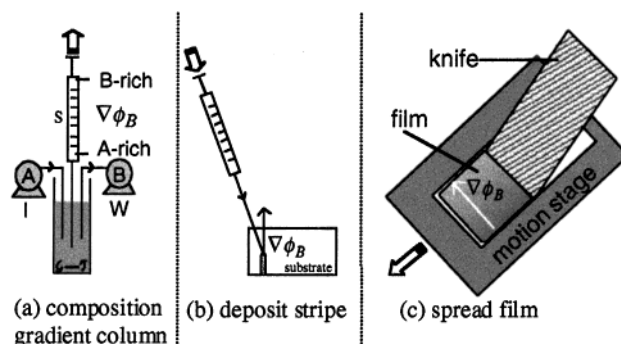*Received March 14, 2000*
Revised Manuscript Received May 31, 2000

Introduction. Because of successes in pharmaceuticals research, combinatorial and high-throughput methods for searching composition space[1−3] have received increasing attention for the synthesis and discovery of new inorganic materials,[4−6] catalysts,[7,8] and organic polymers.[9,10] Combinatorial methods can also allow rapid scanning of parameter space to make fundamental measurements and develop physical models for polymers. One limitation is the difficulty of preparing parallel libraries and performing high-throughput screening with conventional instrumentation and sample preparation. Recently, we developed a combinatorial technique for investigating polymer thin film dewetting phenomena by using sample libraries with orthogonal gradients in thickness and temperature to create a large database of dewetting information in a few hours of experiments.[3,11]

This report describes high-throughput measurement of cloud points for polymer blends utilizing a novel sample deposition method for creating two-dimensional composition (ϕ), temperature (T) libraries. In the sample libraries, T and ϕ are varied orthogonally, and optical microscopy is used to detect phase separation and microstructure. The cloud points determined with this high-throughput method are validated by comparison to conventional light scattering results and single-composition controls.

Library Preparation. Three steps are involved in preparing composition gradient films: gradient mixing (Figure 1a), deposition (Figure 1b), and film spreading (Figure 1c). Two syringe pumps (Harvard PHD2000)[12] (Figure 1a) introduce and withdraw polymer solutions to and from a mixing vial at rates I and W, respectively, where $I = W = 1.7$ mL/min. Pump I contained mass fraction $x_{PS,O} = 0.080$ of polystyrene (PS, $M_r = 96.4$ kg/mol, $M_r/M_n = 1.01$, Tosoh)[13] in toluene. The vial was loaded with an initial $M_0 = 2.0$ mL of mass fraction $x_{PVME,O} = 0.080$ of poly(vinyl methyl ether) (PVME, $M_r = 119$ kg/mol, $M_r/M_n = 2.5$)[14] in toluene from pump W. The infusion and withdrawal syringe pumps were started simultaneously while vigorously stirring the vial solution, and a third syringe, S, was used to manually extract solution from the vial. A mass balance of the transient mixing process gives the mass fraction of PS, x_{PS}, in the vial at any time t (minutes) as

$$x_{PS} = x_{PS,0}\left[\frac{(I - W - S)t + M_0}{M_0}\right]^{-I/(I-W-S)} \tag{1}$$

The mass fraction of PVME in the solution is $x_{PVME} = (1 - x_{PS}/x_{PS,0})x_{PVME,0}$. The relative mass fraction of PS

† Current address: School of Chemical Engineering, Georgia Institute of Technology, Atlanta, GA 30332-0100. E-mail: jcm@che.gatech.edu.

Figure 1. Schematic of the composition gradient film coating procedure.

that will exist in the final coated film (after the solvent dries) is $\phi_{PS} = x_{PS}/(x_{PS} + x_{PVME})$. A volume of 70 μL of the mixing vial contents was sampled for a total of 70 s, beginning 10 s after pumps I and W were started, leading to a predicted range of $0.13 < \phi_{PS} < 0.64$ in the sample syringe and final coated film. Because $I = W$, eq 1 predicts a nonlinear composition gradient, $\phi_{PS} = 0.014t - 9.56 \times 10^{-5}t^2 + 3.68 \times 10^{-7}t^3$, requiring a nonlinear axis scale in plots involving ϕ_{PS}. Using typical values for PS in toluene, the Reynolds number for the sampling syringe is $N_{Re} = Dv\rho/\mu = 0.056$, where $D = 4.2$ mm is the syringe diameter, $v = 0.075$ mm/s is the withdrawal velocity, $\rho = 0.9$ g/cm^3, and $\mu = 0.0047$ Pa·s.[15] In the smaller diameter of the syringe needle, $N_{Re} = 0.3$. Since $N_{Re} < 2100$ in these and all subsequent steps, flow is laminar, preventing turbulent mixing that might perturb the gradient.

Because the sample syringe contains a gradient in the PS and PVME composition along the length of the syringe, molecular diffusion will lead to uniform composition over time. However, the time scale for molecular diffusion is many orders of magnitude larger than the sampling time. The diffusivities of PS and PVME in a PS/PVME/toluene solution with similar molecular mass ($M_r = 110$ kg/mol) and composition as ours have been measured to be $D_{PS} = 3.2 \times 10^{-8}$ cm^2/s and $D_{PVME} = 5 \times 10^{-8}$ cm^2/s.[16] Assuming Fickian diffusion, PS and PVME diffuse in opposite directions in the syringe at 9.3×10^{-11} and 1.5×10^{-10} g/s, respectively.[17] At the point of maximum slope in the ϕ_{PS} gradient (i.e., dϕ_{PS}/d$x = 0.025$ mm^{-1} at $\phi_{PS} = 0.13$), ϕ_{PS} and ϕ_{PVME} change by only 0.004% and 0.001% during the 5 min film deposition process.

Next the gradient solution from the sample syringe is deposited as a thin 31 mm long stripe on the silicon substrate (Figure 1b), at 14 μL/s.[18] The gradient stripe was quickly placed under a stationary knife edge of equal length that was adjusted to be 300 μm above the surface using a micrometer (Figure 1c). The gradient stripe was spread as a film for a distance of 40 mm by moving the substrate under the blade at a velocity of 10 mm/s ($N_{Re} = 0.57$), orthogonal to the composition gradient direction. After a few seconds most of the solvent evaporated, leaving behind a thin film with a gradient of polymer composition. Any remaining solvent was removed during the annealing step. The film thickness, measured with ellipsometry (Filmetrics F20), varied monotonically from 345 to 510 nm between the low and high PS composition ends, due to viscosity
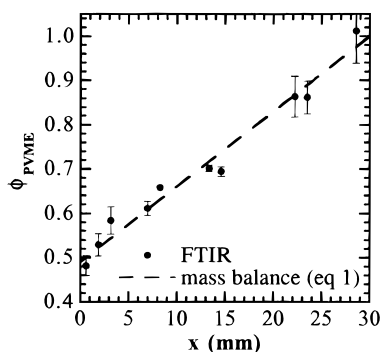
Figure 2. PVME mass fraction calculated from FTIR spectra and compared to prediction from mass balance (eq 1) for the mixing and deposition procedure.

variation in the composition gradient solution. We demonstrated previously that the thickness change due to flow induced by the small thickness gradient ($\approx$5 nm/mm) is within the standard uncertainty of $\pm$3 nm.[11]

By automating the deposition procedure, pump rates were set to values that satisfy $I = (W + S)/2$ to make linear gradients, and the PVME concentration in coated films was measured with FTIR spectroscopy.[19] Spectra demonstrate (not shown) that PVME absorptions increase monotonically with film position, while PS absorptions decrease. The measured ϕ_{PVME} gradient (Figure 2) is linear within standard uncertainty and matches the range and slope predicted by mass balance (eq 1).

High-Throughput Screening. The composition gradient sample was annealed on a linear T gradient heating stage, described elsewhere,[11] over a large range of T values, 90 °C < T < 160 °C. Optical microscope images and photographs capture the phase separation process as a function of T and ϕ_{PS} with average standard uncertainties of $\Delta T = \pm 1.5$ °C and $\Delta\phi_{PS} = \pm 0.006$.

Conventional Cloud Point Measurement. For comparison purposes a HeNe laser light scattering apparatus was used to measure cloud points based upon light scattering at 20° from the incident, from uniform composition and temperature blend samples, 15–20 μm thick, heated at 0.5 °C/min over a range of 120–145 °C. Cloud points were taken as the temperature (with a standard uncertainty of ± 1 °C) where the scattered intensity abruptly increases during heating.

Results and Discussion. Single composition controls subjected to a temperature gradient were used to evaluate the feasibility of proceeding with two-dimensional (T, ϕ_{PS}) gradient measurements. Figure 3a presents a photograph of a 100 nm thick film of mass fraction 20% PS and 80% PVME (near critical composition) annealed over a T gradient. Phase separation above $\approx$140 °C is clearly distinct to the unaided eye compared to the one-phase region below 140 °C. The initial unannealed film had a deep blue color due to reflected light interference effects, identical to the one-phase region in Figure 3a. Optical contrast between homogeneous and heterogeneous regions arises because the optical interference effect is destroyed due to the heterogeneity of phase-separated microstructures. At a thickness of 100 nm the apparent LCST is shifted to higher values than the bulk LCST of 124 °C. Thus, in the remainder of this work we used films with thicknesses high enough to obtain agreement with the bulk LCST cloud point of 124 °C, i.e., greater than $\approx$200 nm. Higher resolution images (Figure 3b) from a 500 nm film with the same composition and T gradient as in Figure
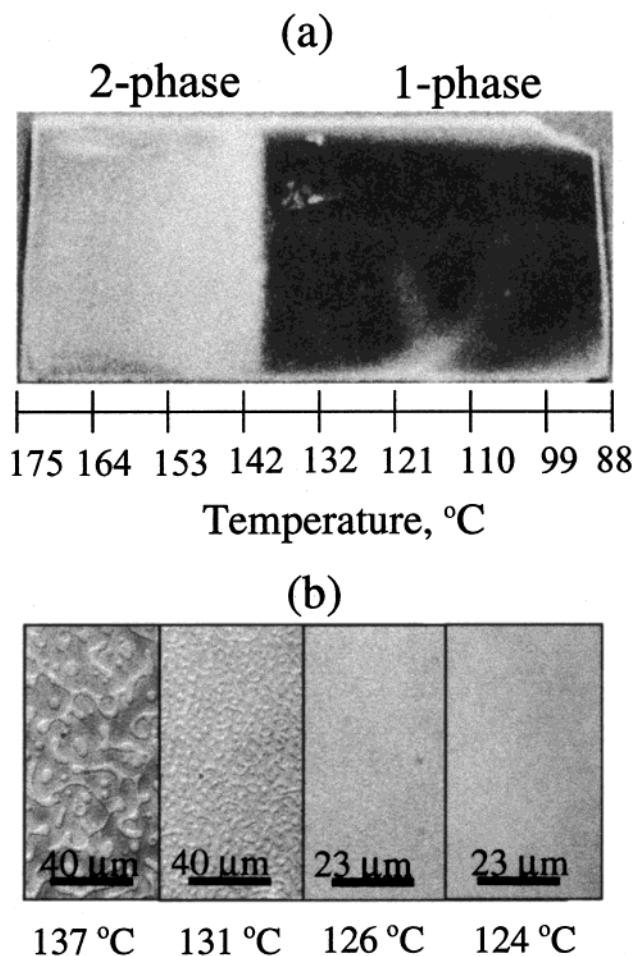

Figure 3. (a) A uniform mass fraction 20% PS/80% PVME film, after annealing over a temperature gradient for 2.5 h. The line separating dark and light regions at 140 °C indicates LCST phase separation above 140 °C. The film thickness is 100 nm, and the film was prepared by spin-coating on a Si–H-coated Si wafer. (b) Higher magnification optical images of selected temperature regions from a 500 nm film annealed on a temperature gradient, as in Figure 2a, for 1 h. The standard uncertainty in the temperature is $\pm$0.8 °C, due to the gradient.

3a demonstrate the expected variation from late-stage breakup into droplets (137 °C) to bicontinuous patterns (131 and 126 °C) to homogeneity (124 °C).

Figure 4 presents a photograph of a typical temperature–composition library after 2 h of annealing, in which the LCST cloud point curve can be seen with the unaided eye. Cloud points measured with conventional light scattering are shown as discrete data points and agree well with the cloud point curve observed on the library. The diffuse nature of the cloud point curves in Figures 3a and 4 reflects the natural dependence of the microstructure evolution rate on temperature and composition, of the type observed in Figure 3b at much higher resolution. Near the LCST boundary the microstructure size *gradually* approaches optical resolution limits (1 μm), giving the curve its diffuse appearance. Based on a bulk diffusion coefficient of $D \approx 10^{-17}$ m^2/s, the diffusion length ($\approx\sqrt{Dt}$) for a 2 h anneal is 270 nm. In Figure 4 each pixel covers $\approx$30 μm, or $\approx$100 times the diffusion length, and gradient-induced diffusion has a negligible effect on the observed LCST cloud point curve.

This study suggests some possible improvements. There is some undulation in the LCST curve and two-phase region in Figure 4 (e.g., the abrupt change in reflectivity that occurs at $\phi_{PS} = 0.35$), presumably due
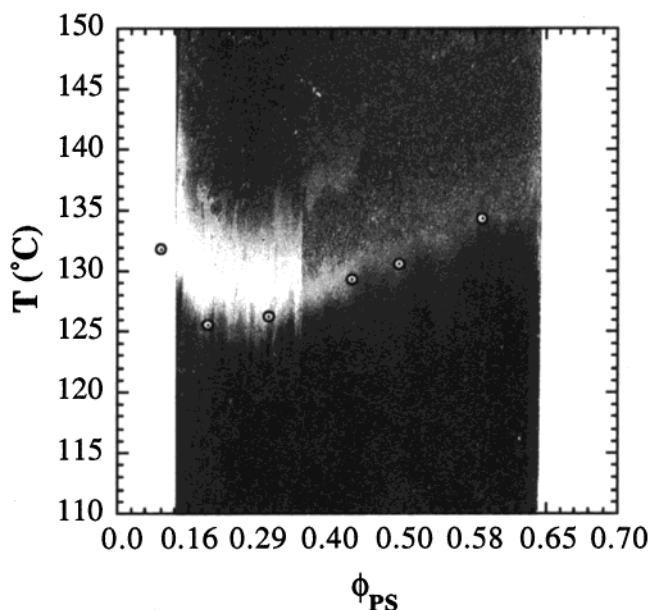
Figure 4. LCST cloud point curve on a two-dimensional PS/PVME blend film library on a Si−H substrate, after 2 h of annealing on the temperature gradient stage. The library cloud point curve agrees well with cloud points (circles with dots) measured independently with laser light scattering. The overall sample dimensions are 30 mm × 40 mm.

to the manual sampling and deposition method used to prepare the Figure 4 sample. These undulations should be correctable by automating the deposition procedure. Although flow in the syringe is laminar, shear in the needle may also induce mixing of the composition gradient, correctable by using larger bore needles. There is some streaking in the microstructure near the cloud point curve, parallel to the T gradient, which may indicate anisotropy introduced during the flow coating process. The use of T and ϕ gradients may also perturb phase behavior or microstructures compared to conventional measurements on uniform samples, on a length scale greater than the diffusion length. One expects an upper limit on the slope of the gradient above which gradients perturb phase behavior. These issues and extensions to additional blend systems are the subject of forthcoming work. In summary, the quantitative FTIR measurements and agreement of the combinatorial-library and uniform-sample cloud point curves validate the novel library deposition and high-throughput approach for mapping polymer blend phase behavior.

References and Notes

(1) Hanak, J. J. *J. Mater. Sci.* **1970**, *5*, 964. Kennedy, K.; Stefansky, T.; Davy, G.; Zackay, V. F.; Parker, E. R. *J. Appl. Phys.* **1965**, *36*, 3808.
(2) Jandeleit, B.; Schaefer, D. J.; Powers, T. S.; Turner, H. W.; Weinberg, W. H. *Angew. Chem., Int. Ed. Engl.* **1999**, *38*, 2494.
(3) Dagani, R. *Chem. Eng. News* **2000**, *78*, 66.
(4) Danielson, E.; Devenney, M.; Giaquinta, D. M.; Golden, J. H.; Haushalter, R. C.; McFarland, E. W.; Poojary, D. M.; Reaves, C. M.; Wenberg, W. H.; Wu, X. D. *Science* **1998**, *279*, 837.
(5) Wang, J.; Yoo, Y.; Gao, C.; Takeuchi, I.; Sun, X.; Chang, H.; Xiang, X.-D.; Schultz, P. G. *Science* **1998**, *279*, 1712.
(6) Reddington, E.; Sapienza, A.; Gurau, B.; Viswanathan, R.; Sarangapani, S.; Smotkin, E.; Mallouk, T. *Science* **1998**, *280*, 1735.
(7) Klein, J.; Lehmann, C. W.; Schmidt, H.-W.; Maier, W. F. *Angew. Chem., Int. Ed. Engl.* **1998**, *37*, 3369.
(8) Bein, T. *Angew. Chem., Int. Ed. Engl.* **1999**, *38*, 323.
(9) Dickinson, T. A.; Walt, D. R.; White, J.; Kauer, J. S. *Anal. Chem.* **1997**, *69*, 3413.
(10) Brocchini, S.; James, K.; Tangpasuthadol, V.; Kohn, J. *J. Biomed. Mater. Res.* **1998**, *42*, 66.
(11) Meredith, J. C.; Smith, A. P.; Karim, A.; Amis, E. J. *Macromolecules*, in preparation.
(12) Certain equipment and instruments or materials are identified in the paper in order to adequately specify the experimental details. Such identification does not imply recommendation by the National Institute of Standards and Technology, nor does it imply the materials are necessarily the best available for the purpose.
(13) According to ISO 31-8, the term "molecular weight" has been replaced by "relative molecular mass," M_r. The number-average molecular mass is given by M_n.
(14) Bauer, B. J.; Hanley, B.; Muroga, Y. *Polym. Commun.* **1989**, *30*, 19.
(15) Budtov, V. P. *Polym. Sci. USSR* **1967**, *9*, 854.
(16) Daivis, P. J.; Pinder, D. N.; Callaghan, P. T. *Macromolecules* **1992**, *25*, 170.
(17) The diffusive flow rate of PS and PVME were calculated as $J = L\pi r^2 D_i\rho(d\phi_i/dx)_{max}$, where ρ is the solution density, $r = 2.3$ mm is the syringe diameter, and $L = 4.2$ mm is the length of the fluid column in the syringe. We estimate $\Delta\phi_i$ as $(Jt)/(x_p L\pi r^2 \rho)$, where $x_p = 0.08$ is the total polymer mass fraction in solution.
(18) To allow for complete wetting by the polymer blend film, the [100] silicon substrates (Polishing Corporation of America) were cleaned in mass fraction 70% H_2SO_4/21% H_2O/9% H_2O_2 at 80 °C for 1.5 h prior to etching 3 min in a HF/NHF$_4$ buffer solution to create a uniform Si−H hydrophobic surface layer.
(19) Spectra were measured with a Nicolet Magna 550 ($\approx$500 μm beam diameter) and were averaged 128 times at 4 cm^{-1} resolution. Films 0.3−1 μm thick were coated on a sapphire substrate, and calibration of the symmetric C−H stretch at 2820 cm^{-1} from the PVME methyl ether group yielded an extinction coefficient of $\epsilon_{2820} = 2.96 \pm 0.04$ abs/(mf μm) where abs = absorbance and mf = mass fraction PVME. The 2820 cm^{-1} absorption was deconvoluted from several nearby peaks using Peakfit (Jandel Scientific).

MA0004662